

NONSINGULAR ROTATING BLACK HOLES IN THE DARK-ENERGY DOMINATED UNIVERSE

RAMÓN TORRES¹

Dept. de Física, Universitat Politècnica de Catalunya, Barcelona, Spain.

Abstract

Motivated by quantum-gravity scenarios that replace the classical black hole singularity with a regular core, and by the possibility that the dark-energy sector may be scale dependent, we construct a broad class of nonsingular rotating black-hole spacetimes embedded in an improved de Sitter-like background with either constant or running Λ . Because the Newman–Janis algorithm is generically incompatible with a cosmological-constant fluid, we instead propose a generalized Kerr–Schild construction on a (possibly scale-dependent Λ) de Sitter seed, yielding a Carter-type metric characterized by a mass function and a Λ function. Our construction provides a direct map from static, spherically symmetric regular models to their rotating counterparts. We derive sharp regularity conditions at the ring and we identify a minimal-order subclass. We analyze chronology and show that, for non-negative mass function and Λ above a certain negative limit, the spacetimes are stably causal. For minimal-order geometries with non-negative mass, we prove that the weak energy condition must be violated. Finally, we illustrate the framework with an asymptotic-safety–inspired model and discuss horizon structure, surface gravities, and conformal diagrams. These results provide a controlled, observationally oriented arena to confront regular rotating black holes in dark-energy backgrounds with the rapidly improving gravitational-wave and horizon-scale imaging data.

KEYWORDS: Rotating black holes; Regular black holes; Quantum black holes; Cosmological constant; Dark energy.

¹E-mail: ramon.torres-herrera@upc.edu

1. INTRODUCTION

According to our present understanding—grounded primarily in General Relativity (GR)—when an astrophysical object’s self-gravity overwhelms all available sources of pressure support, dynamical collapse forms a black hole. Because realistic progenitors generically possess nonzero total angular momentum, conservation of angular momentum implies a spinning remnant; after transient losses through neutrino emission, electromagnetic outflows, and gravitational-wave radiation, the exterior vacuum relaxes, by the black-hole uniqueness results under standard assumptions, to a stationary black hole geometry. Thus, within GR, astrophysical black holes are expected to be rotating black holes (RBHs).

Classical black-hole solutions of general relativity typically exhibit an internal curvature singularity, signaling a breakdown of the classical description. Many authors, therefore, regard the appearance of singularities less as a faithful prediction of nature and more as evidence that the theory is being extrapolated beyond its domain of validity. Motivated by this viewpoint, a substantial body of work has developed singularity-free (regular) black-hole models using complementary effective approaches (see, for example, [1–11] and references therein).

With regard to the background of black holes in the Universe, the standard cosmological model, Λ CDM, assumes the existence of a strictly constant cosmological term Λ in Einstein’s equations (which is responsible for the late-time accelerated expansion of the Universe). Nevertheless, a broad body of work has also explored the possibility of evolving dark-energy using SNe Ia, BAO, CMB, and $H(z)$ measurements. Global analyses generally conclude that dynamical models are not excluded and sometimes mildly preferred, especially when including LSS and bispectrum information [12]. Moreover, recent DESI DR1 BAO measurements provide a dense set of distance indicators over $0.1 \lesssim z \lesssim 3.5$ [13]. While BAO-only constraints remain broadly consistent with Λ CDM, joint analyses with Planck 2018 CMB and type-Ia supernova compilations (e.g. Pantheon+) can favor dynamical dark energy in the (w_0, w_a) framework, with best-fit regions typically drifting toward $w_0 > -1$ and $w_a < 0$ and the cosmological-constant point $(w_0, w_a) = (-1, 0)$ disfavored at the ~ 2.5 – 4σ level in some dataset/priors choices [13–15]. Non-parametric reconstructions using BAO+CMB+SNe similarly report mild departures from a strictly constant dark-energy density over limited redshift ranges [16], although the robustness of these hints remains under scrutiny [15, 17, 18]. Taken together, current data do not rule out Λ CDM, but they motivate exploring theoretically controlled scenarios in which the effective cosmological term is not strictly constant.

On the other hand, from a theoretical point of view, the cosmological constant raises severe theoretical problems: the enormous discrepancy between the observed Λ and naive

quantum-field-theoretic estimates (the *cosmological constant problem*) and the *coincidence problem* of why the vacuum and matter densities are of the same order precisely today [19, 20]. These difficulties motivate scenarios in which the dark energy sector may have dependence on the spacetime point considered. Broadly speaking, dynamical dark energy (DDE) models extend Λ CDM in several directions (for comprehensive reviews see, e.g., [12, 21]): Quintessence and k-essence [22–24], Phantom Scenarios and Model-Independent Parametrizations [12, 25], Interacting dark energy [26], Modified gravity [17, 27], Running vacuum and running cosmological constant [28–30]. In particular, let us highlight running-vacuum models (RVMs) which provide a theoretically motivated realization of dynamical dark energy in which the vacuum term Λ becomes an effective quantity that can vary with cosmological curvature scales, as suggested by QFT in curved spacetime and semiclassical gravity. Recent global fits to pre- and post-DESI-era combinations of SNIa, BAO, $H(z)$, LSS and CMB data indicate that a small level of vacuum dynamics, $|\nu_{\text{eff}}| \sim 10^{-3}–10^{-2}$, can improve the overall likelihood relative to Λ CDM and may help ease the σ_8 and H_0 tensions, though the robustness of these indications are under active scrutiny [13, 14, 29–31].

1.1. THE NEWMAN-JANIS ALGORITHM AND DARK ENERGY

In 1965, Newman and Janis [32] discovered that it was possible to obtain Kerr’s solution by applying an algorithm to a spherically symmetric and static *seed* metric: Schwarzschild’s solution. A significant step towards understanding the algorithm, its possibilities, generalizations and limitations was carried out in [33]. The generalized algorithm allows one to take any static spherically symmetric seed metric and obtain a rotating axially symmetric offspring from it. The application to regular RBH followed [34]: One starts with a regular, static, and spherically symmetric black hole derived from a specific theoretical framework or adopted as a phenomenologically motivated effective model. Then, one applies the generalized Newman-Janis (N-J) algorithm to try to construct a regular RBH.

Unfortunately, the *offspring* has different geometrical properties and also different physical properties. For example, the seed metric can be a perfect fluid, but the offspring will never be another perfect fluid [33]. In this way, if one takes a de Sitter (or anti-de Sitter) spacetime, which can be interpreted as containing a perfect fluid (with density and pressure related by $p = -\rho$), and one applies the algorithm, one does not obtain a solution for a rotating black hole in a background with a cosmological constant ($\mathbf{T} = -\frac{\Lambda}{8\pi}\mathbf{g}$), i.e., Carter’s solution, but a *rotating imperfect fluid* [35]. In fact, the obtained solution has many properties that are not dS/AdS - like [36], such as a different Segré type and the violation of the null energy condition. Therefore, the generalized N-J algorithm does not seem to correctly

generate rotating black hole solutions in a background with a cosmological constant from a spherically symmetric solution.

1.2. GOAL AND STRUCTURE OF THE ARTICLE

Even if a regular RBH model comes from an approach to Quantum Gravity Theory, in this article we will assume that it can be reasonably well described by a manifold endowed with its corresponding metric. Our aim is to find the general metric for a nonsingular rotating black hole embedded in a spacetime with dark energy modelled as a running (or constant) Λ — with Λ acting as an effective local description tied to the curvature/scale of the spacetime. Our metric will accommodate the running Λ consistently, without the artifacts introduced by the N-J algorithm. We will list the conditions required for a good chronological behaviour, analyze the fulfillment of energy conditions and describe its causal structure. We will also propose an alternative algorithm which will provide us with the spacetime geometry for stationary and axially symmetric black holes from static spherically symmetric black hole spacetimes.

This article is organized as follows. In Sec.2 we introduce a generalized Kerr–Schild construction with a (possibly scale-dependent) dark-energy sector, and derive a stationary, axisymmetric metric describing a rotating black hole embedded in a background characterized by a running (or constant) cosmological term. In Sec.3 we formulate and prove the requirements needed to avoid scalar curvature singularities, obtaining necessary conditions on the differentiability and core behavior of the mass function and the running cosmological term. In Sec.4 we prescribe a systematic procedure to promote a given static, spherically symmetric (regular) black-hole model to its rotating counterpart within the class constructed in Sec.2. In Sec.5 we derive the Boyer–Lindquist-like representation of the metric thereby making the relevant hypersurfaces and symmetry structure manifest. In Sec.6 we analyze the chronological properties of the resulting spacetimes, establishing sufficient conditions for stable causality in a natural block decomposition. In Sec.7 we study the stress–energy tensor and show that, for minimal-order regular spacetimes with non-negative mass function, the weak energy condition must be violated. In Sec.8 we characterize the Killing horizons, compute the associated horizon angular velocity and obtain an explicit expression for the surface gravity. In Sec.9 we present an explicit nonsingular rotating black-hole model motivated by asymptotic safety via an RG-improvement prescription, and we discuss its horizon structure and global causal diagram in representative parameter regimes. Finally, Sec.10 summarizes the main results and open problems.

2. METRIC FOR A REGULAR RBH EMBEDDED IN DARK ENERGY

In order to obtain the metric suitable for a regular RBH embedded in dark energy, we will introduce a generalized Kerr-Schild ansatz [36] [37] in which the spacetime metric \tilde{g} for our spacetime \tilde{V} is derived from a seed metric g of a seed spacetime V . The metrics will be related through the relation

$$\tilde{g}_{\alpha\beta} = g_{\alpha\beta} + H l_\alpha l_\beta, \quad (2.1)$$

where both metrics are non-flat, H is a scalar function and l is a null vector with respect to both metrics. A list of some properties of the generalized Kerr-Schild transformation can be found in [36] [37].

Note that this procedure was used in the pioneering work by Carter [38] to obtain a rotating black hole from a seed de Sitter (or AdS) spacetime ($T_{\alpha\beta} = -\Lambda/(8\pi) g_{\alpha\beta}$). This procedure has also been applied recently in the presence of a cosmological constant in [39] and [40]. Nevertheless, the specific procedure in these references is not fully suitable for possibly varying dark energy.

In the general case considered here, our seed metric will be a spacetime containing dynamical dark energy. (The cosmological constant case will be treated as a particular case of the general one). This will be achieved by starting with a de Sitter-like spacetime and allowing Λ to depend on the characteristic scale at which it is probed (and some parameters depending on the chosen approach to dark energy) [41–43]. The line-element for the de Sitter-like spacetime in Carter’s coordinates $\{\tilde{t}, r, \theta, \tilde{\varphi}\}$ takes the form [38]:

$$ds_0^2 = \Sigma \left\{ \frac{dr^2}{(a^2 + r^2) \Psi} + \frac{d\theta^2}{\Delta_\theta} \right\} + \sin^2 \theta \frac{\Delta_\theta}{\Sigma \Xi^2} \left[a d\tilde{t} - (a^2 + r^2) d\tilde{\varphi} \right]^2 - \frac{\Psi (a^2 + r^2)}{\Sigma \Xi^2} \left(d\tilde{t} - a \sin^2 \theta d\tilde{\varphi} \right)^2, \quad (2.2)$$

where we have defined

$$\begin{aligned} \Sigma &\equiv r^2 + a^2 \cos^2 \theta, \\ \Psi &\equiv 1 - \frac{\Lambda r^2}{3}, \\ \Xi &\equiv 1 + \frac{\Lambda a^2}{3}, \\ \Delta_\theta &\equiv 1 + \frac{\Lambda a^2 \cos^2 \theta}{3}. \end{aligned}$$

On the other hand, in the case of applying the Kerr-Schild ansatz to obtain a rotating black hole it is convenient to write the scalar function H as

$$H = \frac{2\mathcal{M}r}{\Sigma},$$

where the scalar function \mathcal{M} is defined as the *mass function*.

We choose the null vector \mathbf{l} in Carter form [38]:

$$l_\alpha dx^\alpha \equiv \frac{d\tilde{t} - a \sin^2 \theta d\tilde{\varphi}}{\Xi} + \frac{\Sigma dr}{\Psi(r^2 + a^2)}, \quad (2.3)$$

which is null with respect to the seed metric (and, thus, to the generated metric) and will provide the required symmetries for \tilde{g} . In this way, from (2.1), the line element derived from the improved de Sitter spacetime will be

$$ds^2 = \Sigma \left\{ \frac{dr^2}{(a^2 + r^2) \Psi} + \frac{d\theta^2}{\Delta_\theta} \right\} + \sin^2 \theta \frac{\Delta_\theta}{\Sigma \Xi^2} [a d\tilde{t} - (a^2 + r^2) d\tilde{\varphi}]^2 - \frac{\Psi (a^2 + r^2)}{\Sigma \Xi^2} (d\tilde{t} - a \sin^2 \theta d\tilde{\varphi})^2 + \frac{2\mathcal{M}r}{\Sigma} \left(\frac{d\tilde{t} - a \sin^2 \theta d\tilde{\varphi}}{\Xi} + \frac{\Sigma dr}{\Psi(r^2 + a^2)} \right)^2, \quad (2.4)$$

where now a acquires a physical interpretation as a rotation parameter that measures the angular momentum per unit of mass [44]. Meanwhile, the scalar functions \mathcal{M} and Λ will depend on both the characteristic scale k at which they are probed (and some parameters depending on the chosen theoretical approach) [41–43]. In this curved spacetime the relevant physical coarse-graining scale is not global and varies from event to event, motivating a local identification $k = k(x)$. In this way, \mathcal{M} and Λ will be functions of the spacetime point considered. However, in order for the spacetime to be stationary and axially symmetric, as we want for our class of rotating black holes, we should impose that the scalar functions \mathcal{M} and Λ can only depend on the coordinates r and θ , so that $\partial_{\tilde{t}}$ and $\partial_{\tilde{\varphi}}$ will be killing vectors associated with the required symmetries².

In the literature the possibility $\mathcal{M}(r, \theta)$ has been treated only in [45] and for a particular case without cosmological constant. Note however, that there are particular cases with $\mathcal{M}(r, \theta)$ and $\Lambda(r, \theta)$ which are interesting from a physical point of view and that will be the focus of future work. In this article we will focus in the case in which \mathcal{M} and Λ only depend on r to make general properties for general functions analytically accessible.

Note that, unlike in the Kerr-de Sitter case, in the case with a varying Λ , Ξ cannot be eliminated by rescaling \tilde{t} and $\tilde{\varphi}$.

The hypersurfaces $r = \text{constant}$ have as their normal $\mathbf{n} = dr$, which satisfies

$$\mathbf{n}^2 = \frac{\Delta_r}{\Sigma},$$

²Note now that the choice of \mathbf{l} makes it invariant under the killing vectors $\partial_{\tilde{t}}$ and $\partial_{\tilde{\varphi}}$, which is key for the derived spacetime to be stationary and axially symmetric.

where

$$\Delta_r \equiv -\frac{\Lambda(r)}{3}r^2(r^2 + a^2) + r^2 - 2\mathcal{M}(r)r + a^2.$$

It can be verified that there are no problems in treating the $r = \text{constant}$ hypersurfaces in Carter's coordinates regardless of the value of Δ_r . In this way, $r = \text{constant}$ is a spacelike hypersurface if $\Delta_r > 0$, timelike if $\Delta_r < 0$ and lightlike if $\Delta_r = 0$ ³.

3. AVOIDING SCALAR CURVATURE SINGULARITIES

We say that there is a *scalar curvature singularity* in a spacetime if any scalar invariant polynomial in the Riemann tensor diverges when approaching it along any incomplete curve. We want our seed de Sitter-like spacetime with metric (2.2) to be devoid of singularities in order for it to be able to generate a singularity-free spacetime. Clearly $\Psi = 0$ is a harmless coordinate singularity, but $\Sigma = 0 \Leftrightarrow (r = 0, \theta = \pi/2)$ could be a scalar curvature singularity. In order to prevent it we have the following

Proposition 1 *Assuming an improved de Sitter metric (2.2) possesses a C^4 function $\Lambda(r)$, a necessary and sufficient condition for its curvature invariants to be finite at $\Sigma = 0$ is*

$$\Lambda'(0) = \Lambda''(0) = \Lambda'''(0) = 0.$$

This can be shown by evaluating the curvature (Ricci) scalar \mathcal{R} near $(r = 0, \theta = \pi/2)$ through a Taylor expansion of Λ . In the expansion one finds terms of the form $\Lambda'(0)/r^2$, $\Lambda''(0)/r^2$ and $\Lambda'''(0)/r$. Therefore, the curvature scalar will only be finite at the ring if $\Lambda'(0) = \Lambda''(0) = \Lambda'''(0) = 0$. If we define $\xi \equiv a \cos \theta / r$ and $\tilde{\xi}$ as its limiting value along a path approaching $(r = 0, \theta = \pi/2)$, the curvature scalar tends to the finite values

$$\mathcal{R} \rightarrow \frac{4a^2 \left(\tilde{\xi}^2 + 1 \right) \Lambda(0)^2 + 12 \left(\tilde{\xi}^2 + 1 \right) \Lambda(0) + 2a^4 \Lambda^{iv}(0)}{(\Lambda(0) a^2 + 3) \left(\tilde{\xi}^2 + 1 \right)},$$

³In the general case treated here one could theoretically have a region with $r_{min} \leq r \leq r_{max}$ where all $r = \text{constant}$ hypersurfaces could be lightlike if the functions \mathcal{M} and Λ satisfy in that region the relation

$$\mathcal{M} = \frac{a^2 + r^2}{2r} \left(1 - \frac{\Lambda}{3} r^2 \right).$$

Clearly, in these regions either Λ and/or \mathcal{M} have to be chosen on purpose to get this behaviour. In this article, these regions will not be considered since there is no physical argument for their existence.

for finite $\tilde{\xi}$, and

$$\mathcal{R} \rightarrow 4\Lambda(0)$$

for $\tilde{\xi}$ infinite. Now, it suffices to examine the finiteness of a full set of invariants like the Carminati-McLenaghan invariants [46] around $(r = 0, \theta = \pi/2)$ with the found conditions for non-singularity to verify that the conditions are in fact necessary and sufficient. The calculations were computed using Maple. \square

Of course, our goal is to get the conditions that a spacetime for the rotating black hole with metric (2.4) should satisfy to be devoid of scalar curvature singularities.

Theorem 1 *Assuming a RBH metric (2.4) possessing a C^3 function $\mathcal{M}(r)$ and a C^4 function $\Lambda(r)$, a necessary condition for its curvature invariants to be finite at $(r = 0, \theta = \pi/2)$ is*

$$\begin{aligned}\mathcal{M}(0) &= \mathcal{M}'(0) = \mathcal{M}''(0) = 0. \\ \Lambda'(0) &= \Lambda''(0) = \Lambda'''(0) = 0.\end{aligned}$$

A metric for a rotating BH satisfying the conditions in the Theorem will be called *scalar-regular* (S-R) metric.

By evaluating the curvature (Ricci) scalar ⁴ \mathcal{R} near the ring through a Taylor expansion of \mathcal{M} and Λ one finds terms of the kind $\Lambda'(0)/r^2$, $\Lambda''(0)/r^2$, $\Lambda'''(0)/r$, $\mathcal{M}'(0)/r^2$ and $\mathcal{M}''(0)/r$. Therefore, the curvature scalar will only be finite at the ring if $\Lambda'(0) = \Lambda''(0) = \Lambda'''(0) = \mathcal{M}'(0) = \mathcal{M}''(0) = 0$. If we define $\xi \equiv a \cos \theta / r$ and $\tilde{\xi}$ as its limiting value along a path approaching the ring, the curvature scalar at the ring tends to the finite values

$$\mathcal{R} \rightarrow \frac{4a^2(\tilde{\xi}^2 + 1)\Lambda(0)^2 + 4(\mathcal{M}'''(0)a^2 + 3\tilde{\xi}^2 + 3)\Lambda(0) + 2\Lambda^{iv}(0)a^4 + 12\mathcal{M}'''(0)}{(\Lambda(0)a^2 + 3)(\tilde{\xi}^2 + 1)},$$

for finite $\tilde{\xi}$, and

$$\mathcal{R} \rightarrow 4\Lambda(0)$$

for $\tilde{\xi}$ infinite. ⁵

On the other hand, if one evaluates the Kretschmann scalar $\mathcal{K} \equiv R_{\alpha\beta\gamma\delta}R^{\alpha\beta\gamma\delta}$ near the ring, one finds a term that behaves as $\mathcal{M}(0)/r^6$. Therefore, to avoid scalar curvature singularities we have to also impose $\mathcal{M}(0) = 0$. If the conditions in the theorem are fulfilled,

⁴Let us remark that the expressions of the all the invariants for this family of spacetimes are extremely complex and lengthy, so that we will only make explicit their expressions when the ring is approached.

⁵Note that, in the absence of Λ , one gets the known results [47] $\mathcal{R} \rightarrow 4\mathcal{M}'''(0)/(\tilde{\xi}^2 + 1)$ for finite $\tilde{\xi}$ and $\mathcal{R} \rightarrow 0$ for infinite $\tilde{\xi}$.

then the Kretschmann scalar takes finite values when the ring is approached. Its limiting expression is too long to be shown here, but it can be verified in the appendix. \square

The soundness of the theorem is confirmed by the Carminati-McLenaghan invariant r_1 (quadratic in the trace-free Ricci tensor: $r_1 = \frac{1}{4}S_{ab}S^{ab}$, where $S_{ab} = R_{ab} - \frac{1}{4}Rg_{ab}$) [46] that, under the assumptions of the theorem takes the finite expression

$$\begin{aligned} r_1 \rightarrow & \frac{1}{(\Lambda(0)a^2 + 3)^2(\tilde{\xi}^2 + 1)^4} \left[\frac{a^8(\tilde{\xi}^2 + \frac{1}{9})(\tilde{\xi}^2 + 1)\Lambda^{iv}(0)^2}{8} \right. \\ & + \frac{(\tilde{\xi}^2 - \frac{1}{3})a^4\mathcal{M}'''(0)\tilde{\xi}^2(\Lambda(0)a^2 + 3)\Lambda^{iv}(0)}{2} \\ & \left. + \mathcal{M}'''(0)^2\tilde{\xi}^4(\Lambda(0)a^2 + 3)^2 \right]. \end{aligned} \quad (3.1)$$

for finite $\tilde{\xi}$ and $r_1 \rightarrow 0$ for infinite $\tilde{\xi}$.⁶

In the same way, the complex Carminati-McLenaghan invariant w_1 (which measures the holomorphic self-dual contraction of the Weyl tensor: $w_1 = \frac{1}{8}(C_{abcd} + i^*C_{abcd})C^{abcd}$) [46] is finite if the conditions of the theorem are fulfilled. Its limiting expression is too long to be shown here, but it can be verified in the appendix.

Therefore, if the necessary differentiability conditions are fulfilled, the mass function and Λ of a scalar-regular black hole should be, respectively, around $r = 0$ of the form $\mathcal{M}(r) = O(r^n)$ with $n \geq 3$ and $\Lambda(r) - \Lambda(0) = O(r^m)$ with $m \geq 4$. A usual case in the literature of regular black holes (without Λ) occurs when $\mathcal{M}(r) = M_3r^3 + O(r^4)$ ($M_3 \neq 0$). If, additionally, $\Lambda(r) - \Lambda(0) = \Lambda_4r^4 + O(r^5)$ ($\Lambda_4 \neq 0$) we will call the spacetime a *minimal-order spacetime*.

4. FROM REGULAR SPHERICALLY SYMMETRIC BHs TO REGULAR ROTATING BHs

Consider a static, spherically symmetric line element with areal radius r ,

$$ds^2 = -f(r)dt^2 + f(r)^{-1}dr^2 + r^2(d\theta^2 + \sin^2\theta d\phi^2), \quad (4.1)$$

where we parametrize

$$f(r) = 1 - \frac{2M(r)}{r} - \frac{\Lambda(r)}{3}r^2, \quad (4.2)$$

⁶Again, in the absence of Λ , one gets, as a subcase, the known results [47] $r_1 \rightarrow \mathcal{M}'''(0)^2\tilde{\xi}^4/(\tilde{\xi}^2 + 1)^4$ for finite $\tilde{\xi}$ and $r_1 \rightarrow 0$ for infinite $\tilde{\xi}$.

with $M(r)$ and $\Lambda(r)$ supplied by an underlying Gravitational Theory (General Relativity, Asymptotic Safety, string-inspired effective gravity, loop-inspired regular black-hole models and so on).

Then we obtain a consistent and computable alternative to Newman–Janis-type constructions for models with a $\Lambda(r)$ sector, within the generalized Kerr–Schild ansatz adopted here, via the following steps:

1. Provided the spherically symmetric model has a function $\Lambda(r)$ satisfying the conditions in Theorem 1, one identifies the function $\Lambda(r)$ for the spherically symmetric model with the function $\Lambda(r)$ for the line element (2.2). In this way, one obtains the metric of a modified de Sitter-like spacetime V which will act as a seed for the RBH spacetime.
2. Using $\Lambda(r)$, one chooses the Kerr–Schild 1-form \mathbf{l} of Carter form (2.3); it is null with respect to the seed metric g and the spacetime metric \tilde{g} by construction.
3. One identifies the mass of the spherically symmetric model as the *mass function* ($\mathcal{M} = M(r)$), provided the spherically symmetric model has a function $M(r)$ satisfying the conditions in Theorem 1.
4. One selects an angular momentum per unit mass a for the rotating black hole and obtains a line element of the type (2.4) by putting together the pieces of the previous steps.

In other words,

Scholium *For any choice of rotation parameter a , the stationary axisymmetric metric (2.4) with the same functions $M(r)$ and $\Lambda(r)$ defines a rotating counterpart within our generalized Kerr–Schild family. Moreover, if M and Λ satisfy the near-ring conditions of Theorem 1, then the resulting rotating geometry is free of scalar polynomial curvature singularities at the ring.*

In Sec. 9, we will apply this procedure to the asymptotic-safety–motivated nonsingular spherically symmetric solutions to construct corresponding families of regular rotating black-hole metrics.

5. BOYER-LINDQUIST-LIKE FORM

When working with general rotating black holes, it is customary to work with the metric expressed in Boyer-Lindquist-like (B-L) form. This is due to various advantages provided by

this form: The symmetries are explicit, it has a near diagonal form (block-diagonalizes the r sector), the key hypersurfaces are simple to identify and so on.

A remark is important here: In general, the B-L form cannot be obtained for \mathcal{M} and Λ depending both on r and θ . Frobenius Theorem implies that only in case we are working with a metric (2.4) in which $\mathcal{M} = \mathcal{M}(r)$ and $\Lambda = \Lambda(r)$, it is possible to transform the line-element (2.4) written in Carter coordinates to a Boyer-Lindquist-like form through a coordinate change $\{\tilde{t}, r, \theta, \tilde{\varphi}\} \rightarrow \{t, r, \theta, \varphi\}$ ⁷ defined through

$$\begin{aligned}\tilde{dt} &= dt + \frac{2\mathcal{M}(r)r\Xi}{\Psi\Delta_r} dr, \\ \tilde{d\varphi} &= d\varphi + \frac{2a\mathcal{M}(r)r\Xi}{(r^2 + a^2)\Psi\Delta_r} dr.\end{aligned}$$

In this way, the line element of the RBH will be rewritten in the Boyer-Lindquist-like form as:

$$ds^2 = \Sigma \left\{ \frac{dr^2}{\Delta_r} + \frac{d\theta^2}{\Delta_\theta} \right\} + \sin^2 \theta \frac{\Delta_\theta}{\Sigma\Xi^2} (adt - (r^2 + a^2)d\varphi)^2 - \frac{\Delta_r}{\Sigma\Xi^2} (dt - a \sin^2 \theta d\varphi)^2. \quad (5.1)$$

As happens in Carter's coordinates (2.2), in order for the angular sector to stay spacelike, $g^{\theta\theta} > 0$ and this leads to the condition $\Delta_\theta > 0$. In this way, a spacelike angular sector implies

$$\Lambda > \Lambda_{min} \equiv \frac{-3}{a^2}, \quad (5.2)$$

which, for a varying Λ , can be interpreted as a limit on how negative Λ can be in the spacetime.⁸

Some examples of well-known BHs that can be obtained by using this procedure are⁹:

- Schwarzschild metric ($M = \text{constant}$, $a = 0$, $\Lambda = 0$),
- Reissner–Nordström metric ($M = m - q^2/(2r)$, $m = \text{constant}$, $q = \text{constant}$, $a = 0$, $\Lambda = 0$),
- Kerr metric ($M = \text{constant}$, $0 < a^2 \leq M^2$, $\Lambda = 0$),
- Kerr-Newman solution ($M = m - q^2/(2r)$, $m = \text{constant}$, $q = \text{constant}$, $a \neq 0$, $a^2 + q^2 \leq M^2$, $\Lambda = 0$),

⁷Note that the usual coordinate change [39] [40] starting from *spheroidal* coordinates to B-L-like coordinates cannot be used if $\Lambda \neq \text{constant}$.

⁸Of course, one can also interpret it as a limit in the rotation parameter, as it is often the case in the literature on the AdS spacetime.

⁹Note that the last two solutions cannot be obtained using the generalized Newman–Janis algorithm.

- Kerr-de Sitter (or Carter) solution ($M = \text{constant}$, $a \neq 0$, $\Lambda > 0$) and Kerr-anti-de Sitter solution ($M = \text{constant}$, $a \neq 0$, $\Lambda < 0$),
- Kerr-Newman-de Sitter solution ($M = m - q^2/(2r)$, $m = \text{constant}$, $q = \text{constant}$, $a \neq 0$, $\Lambda > 0$) and Kerr-Newman-anti-de Sitter solution ($M = m - q^2/(2r)$, $m = \text{constant}$, $q = \text{constant}$, $a \neq 0$, $\Lambda < 0$),

6. CHRONOLOGY

In a time-orientable spacetime, it is natural to require the absence of closed causal curves since the presence of such curves would generate familiar logical paradoxes. A spacetime with no closed causal curves is called *causal* [48]. If, moreover, this property survives under arbitrarily small perturbations of the metric, the spacetime is *stably causal*.

It is well known that the standard maximal analytic extension of the Kerr solution is non-causal. Since the Kerr metric is a special case of (5.1), it is therefore natural to ask whether the maximal extensions of regular rotating black holes (RBH) share this pathology.

As is evident from the transformation between Carter and Boyer–Lindquist (BL) coordinates, in the BL chart the hypersurfaces $r = r_H$ satisfying $\Delta_r|_{r_H} = 0$ correspond to coordinate (not curvature) singularities, as documented in the standard subcases. Consequently, in BL coordinates one works with *blocks*: we call a block *type I* when $\Delta_r > 0$ throughout the block, and *type II* when $\Delta_r < 0$.

Proposition 2 *If $\Xi > 0$ and $r\mathcal{M}(r) > 0$ in a block of type I, then the block is stably causal.*

First, note that $\Xi > 0$ due to the constraints on Λ (5.2). Let us consider the $t = \text{constant}$ hypersurfaces. Their normal 1-form is $\mathbf{n} = dt$ and

$$\mathbf{n}^2 = g^{tt} = -\frac{\Xi^2 F}{\Delta_\theta \Delta_r \Sigma}, \quad (6.1)$$

where

$$F \equiv (a^2 + r^2)^2 \Delta_\theta - \sin^2 \theta a^2 \Delta_r.$$

Note, in particular that, if the specific block contains the ring ($r = 0, \theta = \pi/2$) and there are no scalar curvature singularities then, as the ring is approached, $\mathbf{n}^2 \rightarrow -(1 + \Lambda(0)a^2/3)^3 < 0$).

On the other hand, outside the ring, taking into account the non-negative functions appearing in expression (6.1), $t = \text{constant}$ will be spacelike ($\mathbf{n}^2 < 0$) if, and only if, $F > 0$,

what can be written as

$$(a^2 + r^2)\Sigma\Xi + \sin^2\theta a^2 r\mathcal{M} > 0$$

In this way, if $\Xi > 0$ and the product $r\mathcal{M}(r)$ is non-negative the type I block will have a *function* t with $t = \text{constant}$ spacelike hypersurfaces which, according to proposition 6.4.9 in [48], implies that the block will be stably causal. \square

In the absence of Λ , the condition of a non-negative $r\mathcal{M}(r)$ was already obtained ([49] [50] [51]). Now we find that the limit (5.2) favors the absence of closed timelike curves. The need for this condition is expected since, as deduced from the comments in section 5, the violation of the condition would make the trajectory on a circle having $\theta(\tau) = \tau$, and $\phi(\tau) = \phi_0$ for $\tau \in (0, \pi)$, while $\phi(\tau) = \phi_0 + \pi \pmod{2\pi}$ for $\tau \in (\pi, 2\pi)$ a timelike curve, which will be a *closed* timelike curve.

In the previous proposition (and through the use of $r\mathcal{M}(r)$) we are not excluding the possibility that the spacetime could be extended through the disk with $r < 0$, which would provide a non-topologically trivial spacetime. From a historical point of view, this extension was needed for the singular Kerr solution to solve the problem of differentiability at the disk. Nevertheless, the non-topologically trivial spacetime introduced new problems: closed causal curves (clearly due to the existence of the $r < 0$ regions) and the appearance of conical singularities. In the case treated in this article, where there are no scalar curvature singularities, there are no differentiability problems at the ring. Thus, the extension through the disk with $r < 0$ can be avoided providing a *topologically trivial spacetime* that, moreover, is free of all unphysical behaviours [50] [51]. We can then write the following

Proposition 3 *If $\Xi > 0$ and $\mathcal{M}(r) > 0$ in a block of type I of a nonsingular topologically trivial spacetime, then the block is stably causal.*

Proposition 4 *Blocks of type II are stably causal.*

For these blocks consider the $r = \text{constant}$ hypersurfaces with normal 1-form $\mathbf{n} = dr$ satisfying

$$\mathbf{n}^2 = g^{rr} = \frac{\Delta_r}{\Sigma} < 0.$$

Therefore, there is a *function* r such that the $r = \text{constant}$ hypersurfaces are spacelike. Then, according to proposition 6.4.9 in [48], type II blocks will always be stably causal. \square

7. MINIMAL-ORDER SPACETIMES AND THE WEAK ENERGY CONDITION

The Zero Angular Momentum Observer (ZAMO) is defined by the condition that its conserved axial angular momentum per unit mass vanishes: $L_z = p_\varphi = g_{t\varphi}\dot{t} + g_{\varphi\varphi}\dot{\phi} = 0$, which implies the coordinate angular velocity.

$$\Omega = \frac{d\varphi}{dt} = -\frac{g_{t\varphi}}{g_{\varphi\varphi}} = \frac{a[\Delta_\theta(r^2 + a^2) - \Delta_r]}{F},$$

Associated to these observers we can define the orthonormal tetrad:

$$\begin{aligned}\hat{e}_t &= \sqrt{\frac{\Xi^2 F}{\Delta_r \Delta_\theta \Sigma}} \left(\frac{\partial}{\partial t} + \Omega \frac{\partial}{\partial \varphi} \right), \\ \hat{e}_r &= \sqrt{\frac{\Delta_r}{\Sigma}} \frac{\partial}{\partial r}, \\ \hat{e}_\theta &= \sqrt{\frac{\Delta_\theta}{\Sigma}} \frac{\partial}{\partial \theta}, \\ \hat{e}_\phi &= \sqrt{\frac{\Xi^2 \Sigma}{F \sin^2 \theta}} \frac{\partial}{\partial \varphi}.\end{aligned}$$

The effective density, radial pressure and angular pressures as measured by the ZAMO are defined through $\rho = T_{\mu\nu}e_t^\mu e_t^\nu$, $p_r = T_{\mu\nu}e_r^\mu e_r^\nu$, $p_\theta = T_{\mu\nu}e_\theta^\mu e_\theta^\nu$, $p_\varphi = T_{\mu\nu}e_\varphi^\mu e_\varphi^\nu$, respectively, where the effective energy-momentum tensor is $T_{\mu\nu} \equiv G_{\mu\nu}/(8\pi)$.

Theorem 2 *A rotating minimal-order spacetime with a non-negative mass function must violate the Weak Energy Condition.*

To show this, we must take into account that the existence of a non-negative mass function for a minimal-order case ($M(r) = M_3 r^3 + O(r^4)$ around $r = 0$) requires $M_3 > 0$. On the other hand, consider the ZAMOs located in the rotating axis ($\theta = 0$). It can be verified that for these specific observers $T_{\mu\nu}e_a^\mu e_b^\nu = 0$ if $a \neq b$, i.e., the effective energy-momentum tensor for them is diagonal (or *Type I* [48]). The WEC for type I spacetimes requires (among other inequalities) $\text{WEC}_1 = \rho + p_r \geq 0$ and $\text{WEC}_2 = \rho + p_\theta \geq 0$. Combining these inequalities one gets around $r = 0$:

$$\frac{\text{WEC}_1}{2} + \text{WEC}_2 = -\frac{12M_3}{a^2}r^2 \geq 0,$$

that demands $M_3 < 0$, in contradiction with a positive mass function around $r = 0$. In this way, the WEC cannot be satisfied.

Note that the violation of energy conditions is somehow expected since regularity requires evading at least one hypothesis of the singularity theorems; in effective models this commonly manifests as violation of (some) pointwise energy condition in the high-curvature region.

8. KILLING HORIZONS AND SURFACE GRAVITY

As we have seen in section 2, the isolated $r = r_H$ where $\Delta_r|_H = 0$ are light-like hypersurfaces. These hypersurfaces are generated by the null geodesic congruence tangent to the Killing field [52]

$$\vec{\chi} = \partial_t + \Omega_H \partial_\phi, \quad (8.1)$$

with a specific constant angular velocity

$$\Omega_H = \frac{a}{r_H^2 + a^2}$$

and $\vec{\chi}^2|_H = 0$.

Therefore, using the standard definition, these null hypersurfaces are *killing horizons*. The global behaviour of these horizons allows their classification as Cauchy horizons, event horizons or cosmological horizons. This requires the knowledge of the specific functions $\mathcal{M}(r)$ and $\Lambda(r)$. A particular case will be treated in section 9.

The surface gravity κ in the horizon can be found through [52]

$$\kappa^2 = -\frac{1}{2} \nabla_\mu \chi_\nu \nabla^\mu \chi^\nu,$$

which for our rotating black holes and using the normalization in (8.1) is just

$$\kappa = \frac{\Delta'_r(r_H)}{2(r_H^2 + a^2)\Xi_H},$$

where the prime in Δ' stands for derivative with respect to r . Note that the surface gravity is constant in every horizon.

9. NONSINGULAR RBH MODEL FROM ASYMPTOTIC SAFETY

Weinberg’s asymptotic-safety scenario [53] posits that quantum gravity may be ultraviolet complete due to a non-Gaussian renormalization-group (RG) fixed point, implying a predictive, scale-invariant regime near the Planck scale. In practical functional RG analyses, this idea is often explored within the Einstein–Hilbert truncation, where only the scale dependence of Newton’s coupling ($G(k)$) and the cosmological term ($\Lambda(k)$) is retained [43] [54]. To connect this truncated flow to black-hole spacetimes, one commonly adopts an “RG-improvement” prescription: the classical constants in a metric are replaced by running couplings evaluated at a position-dependent cutoff scale ($k = k(x)$) [6]. While this procedure

has some theoretical support [55], it is not unique and can generate unphysical singularities that reflect the improvement scheme rather than the underlying RG dynamics [56]. For this reason, previous work [57] has derived conditions under which RG improvement yields regular spherically symmetric geometries, focusing on the high-curvature regime where the flow is expected to approach scale invariance and the dynamics are governed by universal data such as critical exponents.

The Einstein-Hilbert subspace is spanned by the dimensionless running Newton coupling

$$g(k) \equiv G(k)k^2,$$

and the dimensionless running cosmological *constant*

$$\lambda(k) \equiv \Lambda(k)k^{-2}.$$

The expansion of their corresponding beta functions around a fixed point in the trans-Planckian regime $\{g_*, \lambda_*\}$ of the RG flow yields [57], to linear order and assuming real critical exponents¹⁰

$$g(k) = g_* + g_1 \left(\frac{k}{M_P} \right)^{-\theta_1} + g_2 \left(\frac{k}{M_P} \right)^{-\theta_2}, \quad (9.1)$$

$$\lambda(k) = \lambda_* + \lambda_1 \left(\frac{k}{M_P} \right)^{-\theta_1} + \lambda_2 \left(\frac{k}{M_P} \right)^{-\theta_2}, \quad (9.2)$$

where θ_i are the critical exponents, g_i and λ_i are parameters and M_P is Planck's mass.

In a spherically symmetric context, the RG-scale takes the form [57]

$$k(r) \simeq \tilde{\xi} M_P r^{-\gamma},$$

where $\tilde{\xi} = \xi(mG_0)^{\gamma-1}/M_P$ and ξ is a positive parameter. By using the Renormalization Group (RG) improvement procedure it was found that the singularity resolution is possible if

$$\gamma \geq 3/2, \quad \lambda_* = 0 \quad \text{and} \quad \theta_i \geq 2$$

are all satisfied. Therefore, $\lambda(k)$ vanishes in the UV and it is dynamically generated by quantum fluctuations as the renormalization group (RG) flow departs from the scale-invariant Planckian regime. Consequently, the macroscopic value of Λ observed at low energies emerges from the renormalization group flow as the energy scale k is lowered, allowing for a physically realistic IR limit Λ_0 .

¹⁰Of course, complex critical exponents are also possible [57] and both cases have been found in the literature, but here we choose the real case to provide an example.

On the other hand, the critical exponents derived in the literature (see, for example, [58–60]) indeed satisfy $\theta_i \sim 2 \pm 0.5$. In this way, the antiscreening character of quantum gravity fluctuations could lead to a sufficient weakening of the gravitational interaction at high curvature scales and might result in regular black holes.

In order to fix a particular model, in this article we choose a minimal model with parameters $\gamma = 3/2$ (which is the most straightforward choice based on physical arguments and dimensional analysis) and $\theta_i = 2$. As a result, by using (9.1) and (9.2), the values of the Newtonian coupling and the running Λ in the UV limit will be, respectively

$$G(r) \simeq \frac{M_P}{m} r^3 [g_* + \Gamma r^3] \text{ and } \Lambda(r) \simeq \Lambda_{UV} = \text{constant}, \quad (9.3)$$

where Γ is a constant. On the other hand, in the IR limit, we should have

$$G(r) \rightarrow G_0 \text{ and } \Lambda(r) \rightarrow \Lambda_0,$$

the standard measured values. To get a model with the correct qualitative features we need interpolating functions between the UV limit and the IR limit. Probably one of the simplest examples could be

$$G(r) = \frac{G_0 r^3}{r^3 + l^3}, \quad (9.4)$$

$$\Lambda(r) = \frac{l^2 + \Lambda_0 r^4}{l^4 + r^4}, \quad (9.5)$$

where $l > 0$ defines the scale separating the UV and the IR behaviour.

$G(r)$ is qualitatively compatible with asymptotic safety (9.3) since around $r = 0$

$$G(r) = \frac{r^3}{l^3} \left(1 - \frac{r^3}{l^3} \right) G_0 + O\left(\frac{r^9}{l^9}\right)$$

and that it satisfies the requirement $G(r \rightarrow \infty) = G_0$. The corresponding mass function is $\mathcal{M}(r) = MG(r)$, where M is the mass of the BH at infinity, which satisfies the conditions for a scalar-regular RBH (theorem 1). Note that this is precisely Hayward's mass function [9].

On the other hand, $\Lambda(r)$ also satisfies the requirement $\Lambda(r \rightarrow \infty) = \Lambda_0$ and it is compatible with asymptotic safety (9.3) and with the non-singularity condition for rotating black holes (theorem 1) since around $r = 0$

$$\Lambda(r) = \Lambda_{UV} + (\Lambda_0 - \Lambda_{UV}) \frac{r^4}{l^4} + O\left(\frac{r^8}{l^8}\right),$$

where $\Lambda_{UV} \equiv 1/l^2$. Note that, in this model if l were of the order of Planck's length then $\Lambda_{UV} \sim 10^{121} \Lambda_0$. In this way, Λ would have its naively *expected* value [19, 20] just in the

interior of the black hole. However, it will decrease due to quantum fluctuations along the RG flow away from the scale invariant regime and towards its observed value in the IR regime.

According to the scholium, a rotating black hole constructed using such functions:

- Satisfies the necessary conditions in Theorem 1 required to avoid scalar curvature singularities. Figures 1 and 2 exemplify this by showing, respectively, the curvature scalar \mathcal{R} and the Kretschmann scalar \mathcal{K} around the ring.

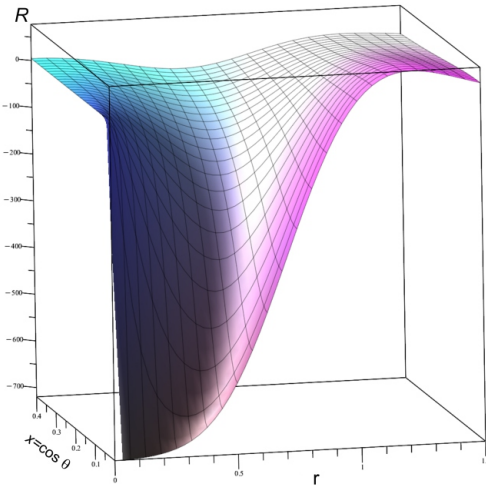


FIGURE 1: *Curvature scalar in the interior region around the ring, where one can explicitly see its finiteness and its directional behaviour at the ring, which corresponds with the one described in the text. For this particular plot the parameters have been chosen as: $l/l_P = 1$, $M/M_P = 10$, $a/M_P = 5$, $\Lambda_0 \cdot l^2 = 0.1$ which, at the ring, provide a maximum value for the curvature scalar $\mathcal{R}_{max} = 4$ and a minimum value $\mathcal{R}_{min} \simeq -720.2857$.*

- Satisfies the conditions in proposition 3 for an asymptotically de Sitter spacetime ($\Lambda_0 > 0$), and therefore, all its blocks will be stably causal.
- Is a *minimal-order* spacetime with a non-negative mass function and has to violate the WECs according to Theorem 2. Figure 3 shows the effective density measured by ZAMO observers which is negative in a region close to the ring. Therefore, it is explicitly shown that the weak energy conditions are indeed violated.

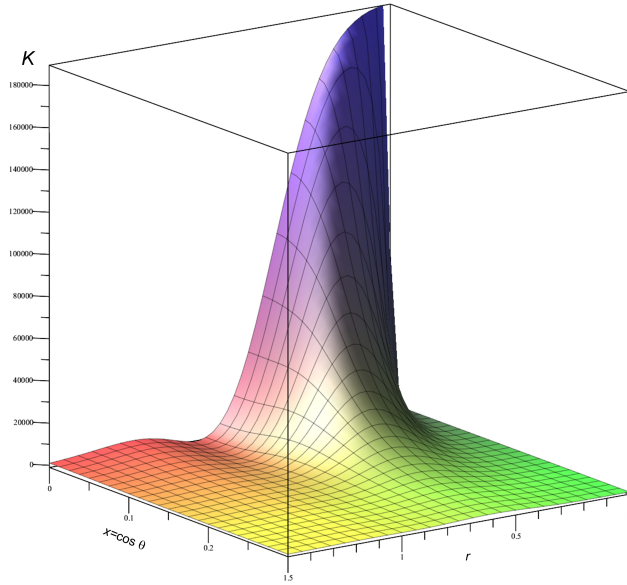


FIGURE 2: *Kretschmann scalar in the interior region around the ring, where one can explicitly see its finiteness and its directional behaviour at the ring, which corresponds with the one described in the text and the expression given in the appendix. For this particular plot the parameters have been chosen as: $l/l_P = 1$, $M/M_P = 10$, $a/M_P = 5$, $\Lambda_0 \cdot l^2 = 0.1$ which, at the ring, provide a maximum value for the Kretschmann scalar $\mathcal{K}_{max} \simeq 189785$ and a minimum value $\mathcal{K}_{min} = 8/3$.*

9.1. HORIZONS AND CAUSAL STRUCTURE

As we have seen, the killing horizons for this family of spacetimes correspond with the isolated zeros $r = r_H$ of Δ_r . It is not possible to find the exact analytical solutions for the zeros of Δ_r . However, it is possible to find them numerically.

Let us first consider the situation in which the effects of Quantum Gravity take place when $l \sim l_P$, the black hole is of astrophysical size ($M \gg M_P$), the angular momentum is small compared to the mass and the IR value of Λ (Λ_0) takes the relatively small values measured in our Universe.

For a classical Kerr-de Sitter black hole of this type, there are three positive horizons: Cauchy horizon (at $r = r_{IH}$), event horizon (at $r = r_{OH}$) and cosmological horizon (at $r = r_C$). In this situation, we expect the quantum corrections to the positions of these horizons to be negligible for the cosmological horizon (since $r_C \gg l$), very small for the event horizon (since $r_{OH} \gg l$) and even relatively small for the Cauchy horizon (since $r_{IH} > l$). Note however that, in the absence of a singularity, now there will not be a *Cauchy horizon*, but an *inner horizon*. The positions of the horizons for a particular case are shown in figure 4.

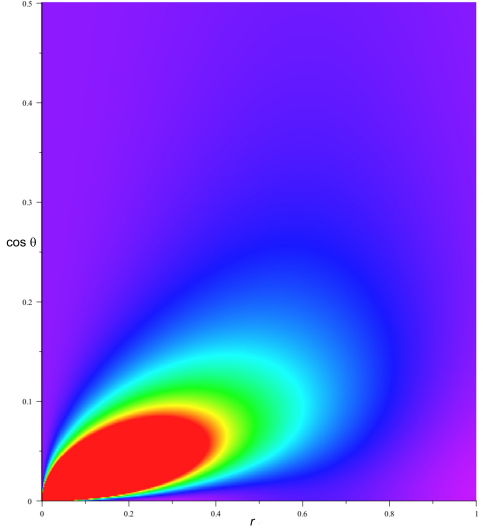


FIGURE 3: A heat map of the effective density as measured by ZAMO observers, where one can explicitly see that there is a region close to the ring where the effective density is mostly negative (red and surrounding non-blue regions). Therefore, the weak energy conditions are violated. For this particular plot the parameters have been chosen as: $l/l_P = 1$, $M/M_P = 10$, $a/M_P = 5$, $\Lambda_0 \cdot l^2 = 0.1$. The minimum value for the effective density is at ($r \simeq 4.0311 \cdot 10^{-4}$, $x = \cos \theta \simeq 5.9911 \cdot 10^{-4}$) where it takes the finite value $\rho \simeq -614682$.

The causal structure of a spacetime corresponding to such a BH is similar to the one corresponding to the classical Kerr-de Sitter solution. The main differences are in the interior of the black hole, where the singularity has been removed and the extension towards negative values of r is no longer needed. The conformal diagram corresponding to such rotating regular BH is shown in figure 5. The existence of horizons divides the figure in blocks of type I and II. We have also differentiated

- Blocks of type Ia as those type I blocks between event horizons r_{OH} and cosmological horizons r_C .
- Blocks of type Ib as those type I blocks between $r = 0$ and the inner horizon r_{IH} .
- Blocks of type IIa as those type II blocks between the event horizon r_{OH} and the inner horizon r_{IH} of the black hole.
- Blocks of type IIb as those type II blocks between the cosmological horizon r_C and infinity.

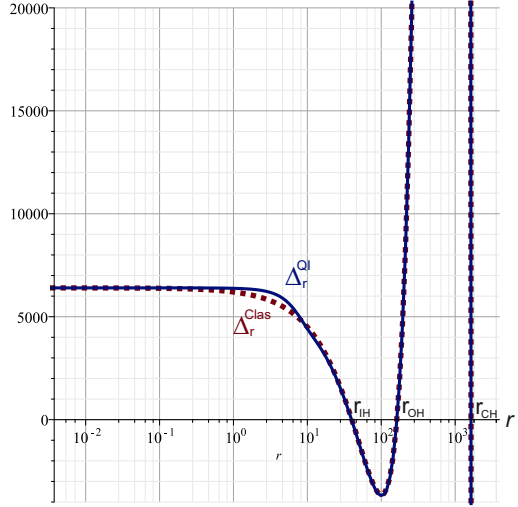


FIGURE 4: A plot of the zeros of Δ_r showing the position of the horizon for the classical (dashed brown) case versus the quantum improved case (solid blue). Note that to improve the visualization, a logarithmic scale has been used in the r axes. It can be verified that, even for $l = G_0 M/10$, the differences between the Δ_r functions are only appreciable in the quantum region below the inner horizon. Specifically, the displacement of the horizons was: $r_{IH} \simeq 0.991 r_{IH}^{Clas}$, $r_{OH} \simeq 1.002 r_{OH}^{Clas}$ and $r_{CH} \simeq 0.9999 r_{CH}^{Clas}$. The particular values used in this plot are $\{l/l_P = 10, M/M_P = 100, a/M_P = 80, \Lambda_0 l_P^2 = 10^{-6}\}$.

On the other hand, only if quantum modifications were of the order of the mass of the black hole ($l \sim M$), a quantum improved black hole could have rather different inner and outer horizons. In this way, if a classical black hole possesses the three typical horizons, its quantum improved counterpart, provided with the same mass, rotation parameter and Λ_0 , could have similar horizons or it could also be an extreme black hole (only a BH horizon and a cosmological horizon) or it could even not be a black hole (hyperextreme case, where only the cosmological horizon remains). This is illustrated in figure 6.

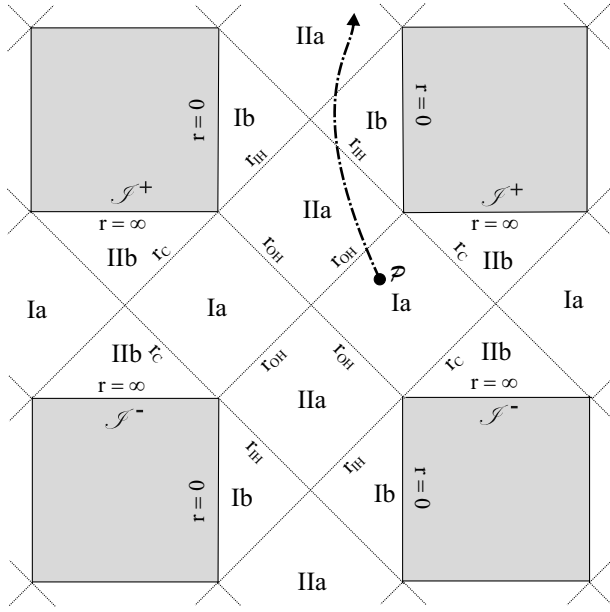


FIGURE 5: A portion of the conformal diagram for the regular rotating black hole.

The grey regions are not part of the spacetime. A test particle initially outside the black hole at point \mathcal{P} can traverse the event horizon and will not reach a singularity. Instead, it could traverse the black hole, as shown. It could even reach the disk at $(r = 0, \theta \neq \pi/2)$ and traverse it (keeping $r(\tau) \geq 0$, $\theta \rightarrow \pi - \theta$ and $\phi \rightarrow \phi + \pi \pmod{2\pi}$), i.e., staying in the Ib region) or reach the ring at $(r = 0, \theta = \pi/2)$, where there are no singularities and continue its travel without any disruption.

10. CONCLUSIONS

Under the working assumption that an effective Lorentzian manifold endowed with a smooth metric provides an adequate description of a regular rotating black hole embedded in a dark-energy environment (i.e., a potentially scale-dependent Λ background), we have constructed the most general stationary and axisymmetric geometry within the generalized Kerr–Schild class studied in this work and analyzed its main geometric and physical properties. Within this framework, the absence of scalar curvature singularities is equivalent to explicit constraints on the differentiability and near-core behaviour of the mass profile $\mathcal{M}(r)$ and of the cosmological term $\Lambda(r)$. We further showed that, under the minimal regularity assumptions adopted here, enforcing scalar regularity generically entails violations of the standard pointwise energy conditions, indicating that effective non-classical stresses are required in the deep interior. Finally, since scalar-regular rotating black holes in our class do not require an extension through the would-be disk, we consistently restrict to a topologically trivial

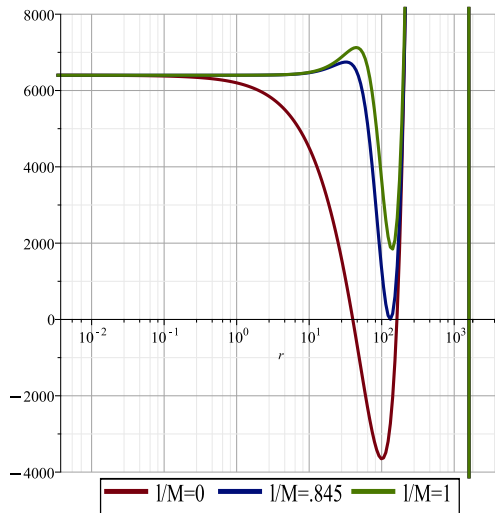


FIGURE 6: A plot of the zeros of Δ_r for significant cases where big quantum corrections are allowed (blue and green curves) versus the classical case (brown curve). In particular, for the value $l/M \simeq 0.845$ (blue curve) the inner horizon and the event horizon of the black hole combine into a single horizon, i.e., one gets an extreme black hole. If the value of l is even bigger the black hole horizons disappear and only the cosmological horizon remains. This is illustrated for $l/M = 1$ (green curve). The particular values used in this plot for the other parameters are $\{M/M_P = 100, a/M_P = 80, \Lambda_0 l_P^2 = 10^{-6}\}$.

spacetime; within this setting, causal pathologies can be excluded under simple sufficient conditions, namely $\mathcal{M}(r) \geq 0$ and $\Lambda(r) \geq -3/a^2$ throughout the domain of interest, which guarantees stable causality in the spacetime.

Since the generalized Newman–Janis algorithm is not directly applicable when a dark-energy sector (equivalently, a cosmological constant or a running Λ -term) is present, in Sec.4 we developed an alternative and fully explicit construction that lifts regular, static, spherically symmetric black-hole models in a dark-energy background to regular rotating spacetimes within our generalized Kerr–Schild framework. This procedure provides a systematic map from the input functions characterizing the seed spherically symmetric solution—in particular the mass profile and the Λ -sector—to the corresponding stationary, axisymmetric geometry, thereby enabling the generation and analysis of broad families of regular rotating black holes beyond the reach of Newman–Janis–type methods.

An essential caveat concerns dynamical stability: our analysis focuses on the stationary geometry and does not assess how perturbations may alter the maximal extension, in particular in the vicinity of the inner (Cauchy) horizon. Inner-horizon instability is well established for Reissner–Nordström (mass inflation) and Kerr spacetimes [61–63]. Most reg-

ular black-hole constructions likewise retain an inner horizon that can be destabilized even by backscattered Hawking flux [64–67], with only finely tuned exceptions [68]. Therefore, a systematic stability analysis across the proposed class of spacetimes—identifying both stable and unstable regimes—constitutes a natural and important direction for future work.

Regarding the observational validation of the models presented here, we emphasize two key aspects:

First, the recent DESI BAO measurements, when combined with CMB and SNe datasets, provide concrete, statistically non-trivial indications that dark energy might be evolving, in qualitative agreement with the expectations of running- Λ scenarios. While Λ CDM remains a viable benchmark model, ongoing and upcoming surveys (DESI extension, Euclid, the Nancy Grace Roman Space Telescope, Rubin/LSST, CMB-S4) will dramatically sharpen the picture. They will either reinforce the case for a running Λ and other forms of DDE or push the allowed level of vacuum dynamics toward zero, providing an unprecedented test of the deepest interface between gravity, quantum theory, and the large-scale structure of the Universe.

Second, rapid progress in black-hole observations—from the LIGO–Virgo–KAGRA gravitational wave network to the Event Horizon Telescope, and soon LISA—is beginning to test theoretical predictions for rotating black holes embedded in dark-energy environments. At the current level of sensitivity and angular resolution, the data remain compatible with both the solutions of General Relativity and a broad class of alternative regular RBH scenarios. However, as measurement precision improves and multi-messenger constraints accumulate, these facilities offer a realistic prospect of discriminating among competing models and of turning the rotating RBH phenomenology discussed here into a quantitatively testable framework.

APPENDIX

When the ring is approached with finite $\tilde{\xi}$ the Kretschmann scalar behaves as

$$\begin{aligned}
\mathcal{K} \rightarrow & \frac{1}{9(\Lambda(0)a^2 + 3)^2(\tilde{\xi}^2 + 1)^6} \left(24\Lambda(0)^2(\Lambda(0)a^2 + 3)^2\tilde{\xi}^{12} \right. \\
& + 24 \left(6\Lambda(0)^2a^2 + (2\mathcal{M}'''(0)a^2 + 18)\Lambda(0) + \Lambda^{iv}(0)a^4 + 6\mathcal{M}'''(0) \right) (\Lambda(0)a^2 + 3)\Lambda(0)\tilde{\xi}^{10} \\
& + \left(360\Lambda(0)^4a^4 + (240\mathcal{M}'''(0)a^4 + 2160a^2)\Lambda(0)^3 \right. \\
& \quad + (120a^6\Lambda^{iv}(0) + 144\mathcal{M}'''(0)^2a^4 + 1440\mathcal{M}'''(0)a^2 + 3240)\Lambda(0)^2 \\
& \quad + (72\Lambda^{iv}(0)a^6\mathcal{M}'''(0) + 360\Lambda^{iv}(0)a^4 + 864\mathcal{M}'''(0)^2a^2 + 2160\mathcal{M}'''(0))\Lambda(0) \\
& \quad \left. + 18\Lambda^{iv}(0)^2a^8 + 216\Lambda^{iv}(0)\mathcal{M}'''(0)a^4 + 1296\mathcal{M}'''(0)^2 \right) \tilde{\xi}^8 \\
& + \left(480\Lambda(0)^4a^4 + (480\mathcal{M}'''(0)a^4 + 2880a^2)\Lambda(0)^3 \right. \\
& \quad + (240a^6\Lambda^{iv}(0) - 48\mathcal{M}'''(0)^2a^4 + 2880\mathcal{M}'''(0)a^2 + 4320)\Lambda(0)^2 \\
& \quad + (96\Lambda^{iv}(0)a^6\mathcal{M}'''(0) + 720\Lambda^{iv}(0)a^4 - 288\mathcal{M}'''(0)^2a^2 + 4320\mathcal{M}'''(0))\Lambda(0) \\
& \quad \left. + 64\Lambda^{iv}(0)^2a^8 + 288\Lambda^{iv}(0)\mathcal{M}'''(0)a^4 - 432\mathcal{M}'''(0)^2 \right) \tilde{\xi}^6 \\
& + \left(360\Lambda(0)^4a^4 + (480\mathcal{M}'''(0)a^4 + 2160a^2)\Lambda(0)^3 \right. \\
& \quad + (240a^6\Lambda^{iv}(0) + 264\mathcal{M}'''(0)^2a^4 + 2880\mathcal{M}'''(0)a^2 + 3240)\Lambda(0)^2 \\
& \quad + (96\Lambda^{iv}(0)a^6\mathcal{M}'''(0) + 720\Lambda^{iv}(0)a^4 + 1584\mathcal{M}'''(0)^2a^2 + 4320\mathcal{M}'''(0))\Lambda(0) \\
& \quad \left. + 84\Lambda^{iv}(0)^2a^8 + 288\Lambda^{iv}(0)\mathcal{M}'''(0)a^4 + 2376\mathcal{M}'''(0)^2 \right) \tilde{\xi}^4 \\
& + \left(144\Lambda(0)^4a^4 + (240\mathcal{M}'''(0)a^4 + 864a^2)\Lambda(0)^3 \right. \\
& \quad + (120a^6\Lambda^{iv}(0) + 96\mathcal{M}'''(0)^2a^4 + 1440\mathcal{M}'''(0)a^2 + 1296)\Lambda(0)^2 \\
& \quad + 96(\Lambda^{iv}(0)a^4 + 6\mathcal{M}'''(0))(\mathcal{M}'''(0)a^2 + \frac{15}{4})\Lambda(0) \\
& \quad \left. + 48\Lambda^{iv}(0)^2a^8 + 288\Lambda^{iv}(0)\mathcal{M}'''(0)a^4 + 864\mathcal{M}'''(0)^2 \right) \tilde{\xi}^2 \\
& + 24\Lambda(0)^4a^4 + (48\mathcal{M}'''(0)a^4 + 144a^2)\Lambda(0)^3 \\
& + (24a^6\Lambda^{iv}(0) + 24\mathcal{M}'''(0)^2a^4 + 288\mathcal{M}'''(0)a^2 + 216)\Lambda(0)^2 \\
& + 24(\mathcal{M}'''(0)a^2 + 3)(\Lambda^{iv}(0)a^4 + 6\mathcal{M}'''(0))\Lambda(0) \\
& \left. + 10\Lambda^{iv}(0)^2a^8 + 72\Lambda^{iv}(0)\mathcal{M}'''(0)a^4 + 216\mathcal{M}'''(0)^2 \right)
\end{aligned}$$

and when the ring is approached with infinite $\tilde{\xi}$ it behaves as $\mathcal{K} \rightarrow (8/3)\Lambda(0)^2$.
When the ring is approached with finite $\tilde{\xi}$ the invariant w_1 behaves as

$$\begin{aligned}
w_1 \rightarrow & \frac{1}{24(\Lambda(0)a^2 + 3)^2(\tilde{\xi}^2 + 1)^6} \left(\right. \\
& (\Lambda^{iv}(0)^2 a^8 + 4\mathcal{M}'''(0)a^6\Lambda^{iv}(0)\Lambda(0) \\
& + (16\mathcal{M}'''(0)^2\Lambda(0)^2 + 12\mathcal{M}'''(0)\Lambda^{iv}(0))a^4 \\
& + 96\Lambda(0)\mathcal{M}'''(0)^2 a^2 + 144\mathcal{M}'''(0)^2) \tilde{\xi}^8 \\
& - 16I(\Lambda(0)a^2 + 3)\mathcal{M}'''(0)(\Lambda^{iv}(0)a^4 + 4\mathcal{M}'''(0)\Lambda(0)a^2 + 12\mathcal{M}'''(0)) \tilde{\xi}^7 \\
& + 4(\Lambda^{iv}(0)a^4 + 3\mathcal{M}'''(0)\Lambda(0)a^2 + 9\mathcal{M}'''(0)) \\
& (\Lambda^{iv}(0)a^4 - 8\mathcal{M}'''(0)\Lambda(0)a^2 - 24\mathcal{M}'''(0)) \tilde{\xi}^6 \\
& + 64I(\Lambda(0)a^2 + 3)^2\mathcal{M}'''(0)^2 \tilde{\xi}^5 \\
& + 6(\Lambda^{iv}(0)a^4 - 2\mathcal{M}'''(0)\Lambda(0)a^2 - 6\mathcal{M}'''(0)) \\
& (\Lambda^{iv}(0)a^4 - \frac{4}{3}\mathcal{M}'''(0)\Lambda(0)a^2 - 4\mathcal{M}'''(0)) \tilde{\xi}^4 \\
& + 16Ia^4(\Lambda(0)a^2 + 3)\mathcal{M}'''(0)\Lambda^{iv}(0) \tilde{\xi}^3 \\
& + 4a^4\Lambda^{iv}(0)(\Lambda^{iv}(0)a^4 + \mathcal{M}'''(0)\Lambda(0)a^2 + 3\mathcal{M}'''(0)) \tilde{\xi}^2 \\
& \left. + \Lambda^{iv}(0)^2 a^8 \right)
\end{aligned}$$

while for infinite $\tilde{\xi}$ it just satisfies $w_1 \rightarrow 0$.

(In the absence of Λ , one gets, as a subcase, the known results [47]

$$w_1 \rightarrow \frac{2\tilde{\xi}^4\mathcal{M}'''(0)^2}{3(1 - I\tilde{\xi})^4(1 + \tilde{\xi}^2)^2}$$

for finite $\tilde{\xi}$ and $w_1 \rightarrow 0$ for infinite $\tilde{\xi}$).

REFERENCES

- [1] Ayon-Beato E and Garcia A 2000 *Phys. Lett. B* **493** 149
- [2] Ayon-Beato E and Garcia A 2005 *Gen. Relativ. Gravit.* **37** 635
- [3] Balart L and Vagenas E C 2014 *Phys. Rev. D* **90** 124045
- [4] Bardeen J M 1968 *Conference Proceedings of GR5* p.174

- [5] Ashtekar A and Bojowald M 2005 *Class. Quantum Grav.* **22** 3349
- [6] Bonanno A and Reuter M 2000 *Phys. Rev. D* **62** 043008 (arXiv:0002196 [hep-th])
- [7] Frolov V P 2014 *JHEP* **5** 049 (arXiv:1402.5446 [hep-th])
- [8] Gambini R and Pullin J 2015 *Proceedings of Science* **14** 038 (arXiv:1408.3050 [gr-qc])
- [9] Hayward SA 2006 *Phys. Rev. Lett.* **96** 031103
- [10] Haggard H M and Rovelli C 2015 *Phys. Rev. D* **92** 104020 (arXiv:1407.0989 [gr-qc])
- [11] Torres R 2014 *Phys. Lett. B* **733** 21
- [12] Avsajanishvili O and Kereselidze T 2022 *Universe* **10** 122
- [13] DESI Collaboration, Adame P et al., 2024 arXiv:2404.03002
- [14] Berghaus K, Orchard SJL and Wiesner M 2024 arXiv:2404.14341
- [15] Roy N 2024 arXiv:2406.00634
- [16] Calderón R et al. 2024 *JCAP* **10** 048 (arXiv:2405.04216 [astro-ph.CO])
- [17] Chudaykin A and Kunz M 2024 arXiv:2407.02558
- [18] Orchard SJL et al. 2024 arXiv:2407.05579 [astro-ph.CO]
- [19] Weinberg S 1989 *Rev. Mod. Phys.* **61** 1
- [20] Carroll SM 2001 *Living Rev. Rel.* **4** 1 (arXiv:astro-ph/0004075)
- [21] Copeland EJ, Sami M and Tsujikawa S 2006 *Int. J. Mod. Phys. D* **15** 1753 (arXiv:hep-th/0603057)
- [22] Caldwell RR and Linder EV 2005 *Phys. Rev. Lett.* **95** 141301 (arXiv:astro-ph/0505494)
- [23] Linder EV 2008 *Gen. Relativ. Gravit.* **40** 329 (arXiv:0704.2064)
- [24] Tsujikawa S 2013 *Class. Quantum Grav.* **30** 21 214003
- [25] Bahamonde S, Böhmer CG, Carloni S, Copeland EJ, Fang W and Tamanini N 2018 *Phys. Rept.* **775** 1 (arXiv:1712.03107 [gr-qc])
- [26] Wang B, Abdalla E, Atrio-Barandela F and Pavon D 2016 *Rept. Prog. Phys.* **79** 9 096901 (arXiv:1603.00331 [astro-ph.CO])

- [27] Nojiri S, Odintsov SD and Oikonomou VK 2017 *Phys. Rept.* **692** 1 (arXiv:1705.11098 [gr-qc])
- [28] Shapiro IL and Solà J 2009 *Phys. Lett. B* **682** 105 (arXiv:0910.4925)
- [29] Solà-Peracaula J 2022 *Phil. Trans. Roy. Soc. A* **380**, 20210182 (arXiv:2203.13757)
- [30] Moreno-Pulido C, Solà-Peracaula J and Cheraghchi S 2023 *Eur. Phys. J. C* **83** 637 (arXiv:2301.0525 [gr-qc])
- [31] Solà-Peracaula J, Gómez-Valent A, de Cruz-Perez J and Moreno-Pulido C 2023 *Universe* **9** 262 (arXiv:2304.11157)
- [32] Newman, E T and Janis A I 1965 *J. Math. Phys.* **6** 915
- [33] Drake S P and Szekeres P 2000 *Gen. Relativ. Gravit.* **32** 445
- [34] Bambi C and Modesto L 2013 *Phys. Lett. B* **721** 329 (arXiv:1302.6075 [gr-qc])
- [35] Azreg-Aïnou M 2014 *Phys. Rev. D* **90** 064041 (arXiv:1405.2569 [gr-qc])
- [36] Bilge AH and Gürses M 1983. *Generalized Kerr-Schild transformation*. Serdaroglu, M., İnönü, E. (eds) Group Theoretical Methods in Physics. Lecture Notes in Physics, vol 180. Springer, Berlin, Heidelberg.
- [37] Kramer D, Stephani H, Herlt E and MacCallum M 1980 *Exact Solutions of Einstein's Field Equations*, Cambridge University Press, Cambridge
- [38] Carter B 2009 *Gen. Relativ. Gravit.* **41** 2873 <https://doi.org/10.1007/s10714-009-0888-5> (Republication of: Black hole equilibrium states (1973))
- [39] Gibbons GW, Lü H, Page DN and Pope CN 2005 *Journal of Geometry and Physics* **53** 49 (arXiv:0404008 [hep-th])
- [40] Neves JCS and Saa A 2014 *Phys. Lett. B* **734** 44
- [41] Wilson K G and Kogut J 1974 *Phys. Rep.* **12** 75
- [42] Weinberg S 1979 *Ultraviolet divergences in quantum theories of gravitation*, in General Relativity: An Einstein Centenary Survey, eds. S. W. Hawking and W. Israel, Cambridge University Press, pp. 790–831.
- [43] Reuter M 1998 *Phys. Rev. D* **57**(2) 971

- [44] Misner CW, Thorne KS and Wheeler JA 1970 *Gravitation*, W.H. Freeman and Company, New York
- [45] Eichhorn A and Held A 2021 *JCAP* **05** 073 (arXiv:2103.13163 [gr-qc])
- [46] Carminati J and McLenaghan RG 1991 *J. Math. Phys.* **32** 3135
- [47] Torres R and Fayos F 2017 *Gen. Relativ. Gravit.* **49** 2 (arXiv:1611.03654 [gr-qc])
- [48] Hawking SW and Ellis GFR 1973 *The large scale structure of space-time* Cambridge University Press, Cambridge
- [49] Maeda H 2021 (arXiv:2107.04791 [gr-qc])
- [50] Torres R 2023 *Phys. Rev. D* **108** 084008 (arXiv:2307.12096 [gr-qc])
- [51] Torres, R 2025 *Gen. Relativ. Gravit.* **57** 50 (arXiv:2407.14851 [gr-qc])
- [52] Wald RM 1984 *General Relativity* Chicago : University of Chicago Press
- [53] Weinberg S 1972 *Gravitation and Cosmology: Principles and applications of the general theory of relativity* New York: John Wiley & Sons.
- [54] Reuter M and Saueressig F 2002 *Phys. Rev. D* **65** 065016
- [55] Borissova JN and Platania A 2023 *J. High Energ. Phys.* **2023** 46.(arXiv:2210.01138 [gr-qc])
- [56] Koch B and Saueressig F 2014 *Class. Quantum Grav.* **31** 015006
- [57] Adéiféoba A, Eichhorn A and Platania A 2018 *Class. Quantum Grav.* **35** 225007 (arXiv:1808.03472 [gr-qc])
- [58] Benedetti D, Machado PF and Saueressig F 2009 *Mod. Phys. Lett. A* **24** 2233 (arXiv:0901.2984 [hep-th])
- [59] Gies H, Knorr B and Lippoldt S 2015 *Phys. Rev. D* **92** 084020 (arXiv:1507.08859 [hep-th])
- [60] Donà P, Eichhorn A and Percacci R 2014 *Phys. Rev. D* **89** 084035 (arXiv:1311.2898 [hep-th])
- [61] Poisson E and Israel W 1990 *Phys. Rev. D* **41** 1796

- [62] Bernard FW 1989 *J. Math. Phys.* **30** 1301
- [63] Poisson E and Israel W 1989 *Phys. Rev. Lett.* **63** 1663
- [64] Torres R 2013 *Phys. Lett. B* **724** 338 (arXiv:1309.1083 [gr-qc])
- [65] Carballo-Rubio R, Di Filippo F, Liberati S, Pacilio C and Visser M 2018 *JHEP* **07** 023 (arXiv:1805.02675 [gr-qc])
- [66] Carballo-Rubio R, Di Filippo F, Liberati S, Pacilio C and Visser M 2021 arXiv: 2101.05006 [gr-qc]
- [67] Carballo-Rubio R, Di Filippo F, Liberati S, Pacilio C and Visser M 2022 arXiv: 2205.13556 [gr-qc]
- [68] Franzin E, Liberati S, Mazza J and Vellucci V 2022 arXiv:2207.08864 [gr-qc]